Thermochimica Acta, 150 (1989) 63–78
Elsevier Science Publishers B.V., Amsterdam – Printed in The Netherlands

THERMAL DECOMPOSITION KINETICS. PART XVI. KINETICS AND MECHANISM OF THERMAL DECOMPOSITION OF DIAQUOBIS(ETHYLENEDIAMINE)COPPER(II) OXALATE

C.G.R. NAIR and SURESH MATHEW

Department of Chemistry, University of Kerala, Trivandrum 695034 (India)

K.N. NINAN

Analytical and Spectroscopy Division, SPPC, Vikram Sarabhai Space Centre, Trivandrum 695022 (India)

(Received 18 January 1989)

ABSTRACT

The kinetics and mechanism of thermal decomposition of diaquobis(ethylenediamine)copper(II) oxalate were studied using non-isothermal thermogravimetry (TG) and differential scanning calorimetry (DSC). The stages of decomposition were identified from TG/DTG, independent pyrolysis and X-ray diffraction data. The complex undergoes a three-step decomposition corresponding to dehydration, deamination to mono(amine) complex followed by simultaneous deamination, and decomposition giving rise to copper(II) oxide. The kinetic parameters for the three steps of decomposition were calculated from the TG and DSC curves using four integral methods. The rate-controlling process for all three stages of decomposition is random nucleation with the formation of one nucleus on each particle (Mampel equation). The heat of reaction for each stage of decomposition was determined using DSC.

INTRODUCTION

Kinetics of thermal dehydration of different complexes and salts have been extensively studied recently. Both isothermal and non-isothermal methods have been used to evaluate the mechanism of dehydration reactions [1–3]. These studies have so far been confined largely to thermal dehydrations. A search through the literature showed that very few attempts have been made to undertake a study of the kinetics of thermal deamination [4,5]. Although transition metal amine complexes were known for a long time, investigations on their thermal decomposition behaviour have been carried out only recently [6].

In an earlier publication we reported the kinetics and mechanism of thermal decomposition of a complex containing a monodentate ligand [7]. It

0040-6031/89/$03.50

was considered worthwhile to investigate the thermal decomposition of a transition metal complex containing a bidentate ligand. The major objectives of this investigation were to study the data obtained from non-isothermal TG and DSC curves of diaquobis(ethylenediamine)copper(II) oxalate and to evaluate the kinetic parameters for the different stages of decomposition, and to shed light on the mechanism of the thermal degradation. We also attempted to evaluate the heats of reaction for the different stages of thermal decomposition from the DSC curves.

EXPERIMENTAL

Synthesis of diaquobis(ethylenediamine)copper(II) oxalate

The $[Cu(en)_2(H_2O)_2]C_2O_4$ was prepared by the addition of an excess of ethylenediamine to solid copper oxalate hemihydrate, followed by the addition of enough water to effect solution [8]. The dark-purple-coloured solution was filtered and acetone was added to the filtrate to cause crystallization of the complex. After filtration, the crystals were washed with acetone and dried in vacuo over phosphorus(V) oxide. The resulting complex was characterized by spectral and chemical methods. The copper content in the complex was analysed gravimetrically. Microanalysis of carbon, hydrogen and nitrogen was done at the Central Drug Research Institute, Lucknow. The results of the analysis are given in Table 1.

Instruments

Simultaneous TG–DTG curves were recorded using a DuPont 990 thermal analyser in conjunction with a 951 thermogravimetric analyser. DSC analysis was carried out using the Mettler TA 3000 thermal analysis system. The experiments were carried out in nitrogen atmosphere at a flow rate of 50 $cm^3\ min^{-1}$. The sample mass was 10 ± 0.2 mg and the heating rate was $10\,^\circ C\ min^{-1}$. DSC curves were recorded using an open cup sample holder. The X-ray powder diffractograms were recorded using a Philips 1710

TABLE 1

Analytical results for $[Cu(en)_2(H_2O)_2]C_2O_4$

	Theoretical (%)	Observed (%)
Copper	20.66	20.33
Carbon	23.41	22.95
Hydrogen	6.55	6.47
Nitrogen	18.20	17.68

diffractometer with a PW1729 X-ray generator using Co Kα radiation. Computational work was done with an IBM-PC/XT using the FORTRAN 77 program.

MATHEMATICAL TREATMENT OF DATA

Kinetic parameters were calculated from the TG and also from DSC curves using four non-mechanistic methods. The forms of these equations used are given below where a term $g(\alpha)$, has been introduced for convenience and is defined as

$$g(\alpha) = \frac{1-(1-\alpha)^{1-n}}{1-n} \quad \text{where} \quad \alpha_t = \frac{m_t}{m_\infty} = \frac{a_t}{a_\infty}$$

Coats–Redfern equation [9]

$$\ln\left[\frac{g(\alpha)}{T^2}\right] = \ln\left[\frac{AR}{\phi E}\left(1-\frac{2RT}{E}\right)\right] - \frac{E}{RT} \tag{1}$$

MacCallum–Tanner equation [10]

$$\log_{10} g(\alpha) = \log_{10}\left(\frac{AE}{\phi R}\right) - 0.485E^{0.435} - \frac{[0.449+0.217E]\times 10^3}{T} \tag{2}$$

Horowitz–Metzger equation [11]

$$\ln\ g(\alpha) = \ln\left(\frac{ART_s^2}{\phi E}\right) - \frac{E}{RT_s} + \frac{E\theta}{RT_s^2} \tag{3}$$

MKN equation [12]

$$\ln\left(\frac{g(\alpha)}{T^{1.9215}}\right) = \ln\left(\frac{AE}{\phi R}\right) + 3.7721 - 1.9215\ \ln\ E - 0.12039\left(\frac{E}{T}\right) \tag{4}$$

where α = fractional decomposition, n = order parameter, T = temperature (K), A = pre-exponential factor, ϕ = heating rate in °C min^{-1}, E = energy of activation, R = gas constant, T_s = DTG peak temperature, $\theta = T - T_s$, m = mass loss in TG experiment, and a = area of DSC curve at time t and after completion of the reaction.

Determination of order parameter n

The order parameter n was evaluated for the different stages of decomposition using the Coats–Redfern equation by an iteration method. Using a computer, linear plots of $\ln[g(\alpha)/T^2]$ versus $1/T$ were drawn using the least-squares method, taking the α and corresponding T values from the TG curve. Linear curves were drawn for different values of n ranging from 0

to 2, in increments of 0.01. The value of n which gave the best fit was chosen as the order parameter for each stage of decomposition.

The kinetic parameters were calculated from the linear plots of the left-hand side of the kinetic equations against $1/T$ for eqns. (1), (2) and (4), and against θ for eqn. (3). The values of E and A were calculated from the slope and intercept, respectively.

The entropy of activation was calculated from the equation

$$A = \left(\frac{kT_s}{h}\right) \exp\left(\frac{\Delta S}{R}\right)$$

where k = Boltzmann constant, h = Planck's constant, and ΔS = entropy of activation. The heat of reaction ΔH was evaluated by the DSC curve–peak integration.

Mechanism of reaction from non-isothermal TG

Deduction of the mechanism of reactions from non-isothermal methods has been discussed by Sestak and Berggren [13]. Kinetic parameters are evaluated from non-isothermal TG curves by the application of the Arrhenius equation

$$\frac{d\alpha}{f(\alpha)} = \frac{A}{\phi} e^{-E/RT} dT$$

The usual non-mechanistic kinetic equations are mere extensions of those used in homogenous kinetics, where it is assumed that $f(\alpha) = (1-\alpha)^{1-n}$. In contrast, mechanistic kinetic studies are based on the assumption that the

TABLE 2

Mechanism-based equations

Equation	Form of $g(\alpha)$	Rate-controlling process
1	α^2	One-dimensional diffusion
2	$\alpha + (1-\alpha)\ln(1-\alpha)$	Two-dimensional diffusion
3	$[1-(1-\alpha)^{1/3}]^2$	Three-dimensional diffusion, spherical symmetry; Jander equation
4	$(1-2/3\alpha)-(1-\alpha)^{2/3}$	Three-dimensional diffusion, spherical symmetry; Ginstling–Brounshtein equation
5	$-\ln(1-\alpha)$	Random nucleation, one nucleus on each particle; Mampel equation
6	$[-\ln(1-\alpha)]^{1/2}$	Random nucleation; Avrami equation I
7	$[-\ln(1-\alpha)]^{1/3}$	Random nucleation; Avrami equation II
8	$1-(1-\alpha)^{1/2}$	Phase boundary reaction, cylindrical symmetry
9	$1-(1-\alpha)^{1/3}$	Phase boundary reaction, spherical symmetry

form of $f(\alpha)$ depends on the reaction mechanism. A series of $f(\alpha)$ forms are proposed and the mechanism is obtained from the one that gives the best representation of the experimental data.

In this study, kinetic parameters are calculated using the integral method. The integral forms of

$$\int_0^a \frac{d\alpha}{f(\alpha)} = g(\alpha)$$

for nine probable reaction mechanisms, listed by Satava [14], are given in Table 2. The Coats–Redfern method was used for solving the exponential integral, because it is one of the best approaches recommended by several authors [15–17].

Linear plots of the nine forms of $g(\alpha)/T^2$ versus $1/T$ were drawn by the least-squares method, and the corresponding correlation coefficients were also evaluated. E and A were calculated in each case from the slope and intercept, respectively.

RESULTS AND DISCUSSION

For $[Cu(en)_2(H_2O)_2]C_2O_4$, the TG curve (Fig. 1) shows three stages of decomposition. The values of the temperature of inception, T_i, temperature of completion of reaction, T_f, and the DTG peak temperature, T_s, for each stage of decomposition, and the mass loss data are given in Table 3. The results obtained from independent pyrolysis agree well with the TG data.

The compound begins to lose mass at 70 °C. The first mass loss, which resulted in a break in the curve at 105 °C, corresponds to the loss of two molecules of water to form $[Cu(en)_2]C_2O_4$. A well-defined plateau was observed, indicating that the bis(ethylenediamine) complex is quite stable. The second stage corresponds to the evolution of one molecule of ethylenediamine to form the mono(amine) complex. The last stage involves the decomposition of the mono(amine) complex to copper oxide. (No clear-cut stage representing the intermediate formation of anhydrous metal oxalate was observed.) A very small mass loss, indicated in the TG curve in the temperature range 25–40 °C, is due to the evolution of adsorbed moisture. This is also shown as small humps in the DTG and DSC curves.

The different stages of decomposition are given below:

Stage I

$$[Cu(en)_2(H_2O)_2]C_2O_4(s) \rightarrow [Cu(en)_2]C_2O_4(s) + 2H_2O(g)$$

Stage II

$$[Cu(en)_2]C_2O_4(s) \rightarrow Cu(en)C_2O_4(s) + en(g)$$

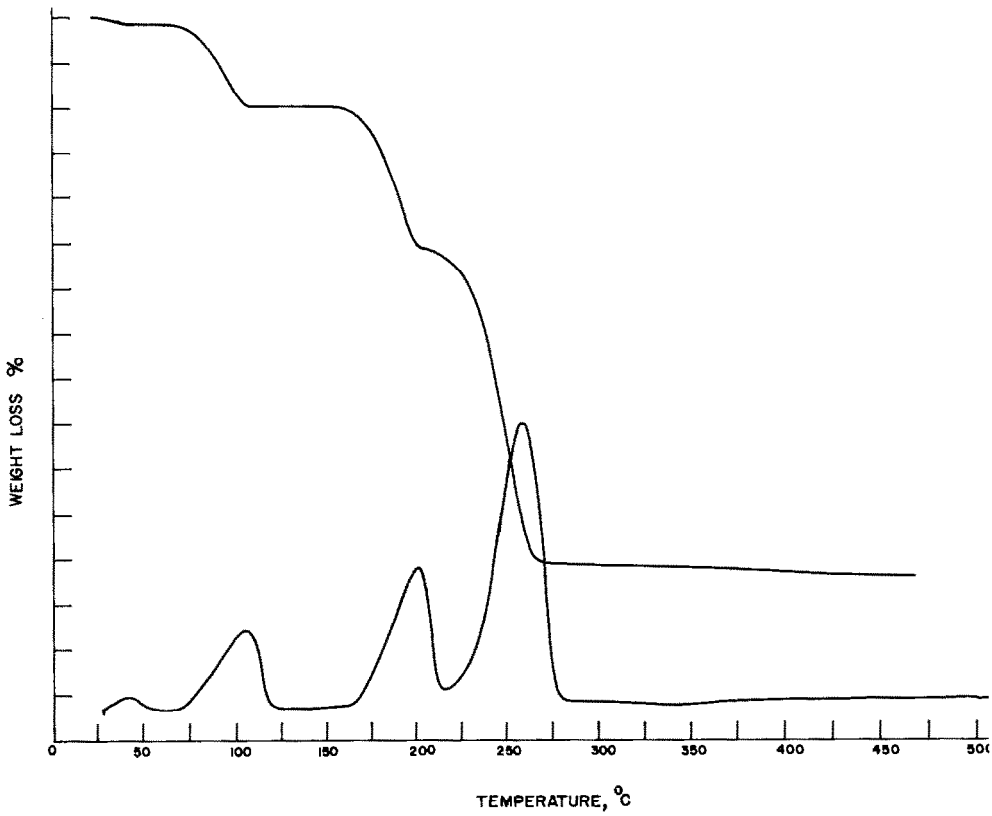

Fig. 1. TG and DTG curves of $[Cu(en)_2(H_2O)_2]C_2O_4$.

Stage III

$$Cu(en)C_2O_4(s) \rightarrow CuO(s) + en(g) + CO_2(g) + CO(g)$$

The reactions observed in the decomposition of $[Cu(en)_2(H_2O)_2]C_2O_4$ are found to be somewhat similar to those previously reported [8]. The first-stage mass loss results in the formation of $[Cu(en)_2]C_2O_4$. This compound could be a square planar product formed by the decomposition of the original hydrated complex having octahedral geometry. Usually in bis(ethylenediamine) complexes, the copper(II) ion will occupy an essentially tetragonal environment, with the ethylenediamine ligands coordinating to form a square coplanar structure with the methylene groups of the ligand occupying a gauche configuration [18]. The formation of the mono(amine) complex is inconsistent with the earlier observations [8]. This may be because of the change in atmosphere (from static air to dynamic nitrogen and hence the oxidation of the relatively unstable intermediate). Since copper(II) usually has a coordination number four, this product could be formed by an anation reaction [19].

TABLE 3

Phenomenological data for the thermal decomposition of diaquobis(ethylenediamine)copper(II) oxalate

Stage	Decomposition mode	TG results					Independent pyrolysis		
		T_i (°C)	T_f (°C)	T_s (°C)	% wt. loss		% wt. loss		Residue
					Theoretical	Observed	Theoretical	Observed	
I	Loss of two H_2O	70	105	99	11.70	11.39			
II	Loss of one en	160	205	190	19.51	19.62			
III	Decomposition of $Cu(en)C_2O_4$	207.5	272.5	250	42.92	43.67	74.13	74.37	CuO

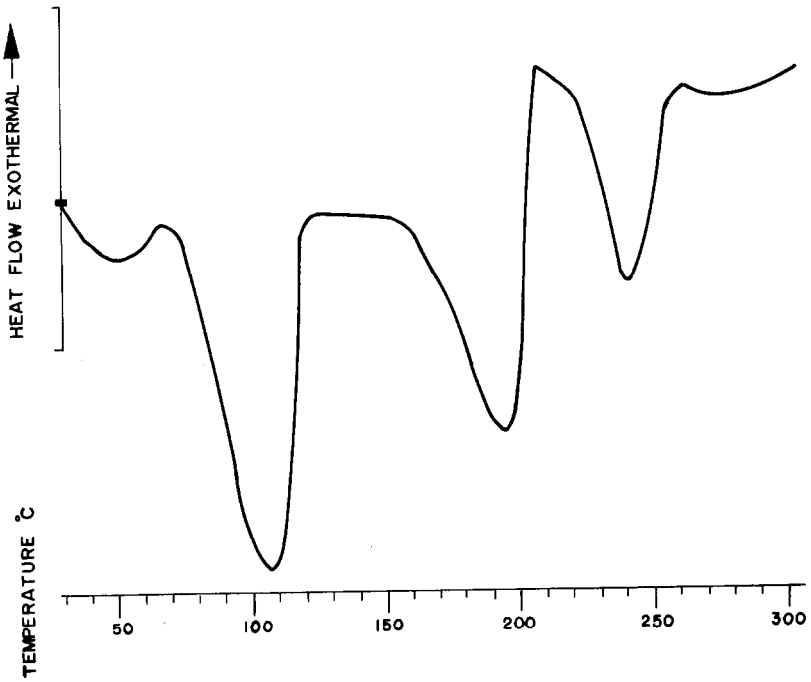

Fig. 2. DSC curve of $[Cu(en)_2(H_2O)_2]C_2O_4$.

A typical DSC curve for the complex is shown in Fig. 2. The three endothermic peaks correspond to the three stages of decomposition of the complex, given above. The values for T_i, T_f and T_s (i.e. T_{max}) for each stage of decomposition are shown in Table 4. The first peak, with a T_s value of 110 °C, is due to the dehydration reaction; the second endothermic peak, with a T_s value of 300 °C, is due to the bis → monoamine transition; while the third endothermic peak is due to the decomposition of the mono(ethylenediamine) complex.

A comparison of the powder diffractograms with the JCPDS powder diffraction file [20] has shown that the final residue obtained is copper(II) oxide. The intermediates of the above decomposition stages were prepared by keeping the complex in a muffle furnace at the appropriate temperatures.

TABLE 4

Endothermic reaction temperatures and ΔH of the thermal decomposition of $[Cu(en)_2(H_2O)_2]C_2O_4$ from DSC curves

Stage	T_i (°C)	T_s (°C)	T_f (°C)	ΔH (J g^{-1})
I	65.7	105.0	127.0	344.29
II	150	194.8	208.0	327.66
III	208	240.0	264.0	154.22

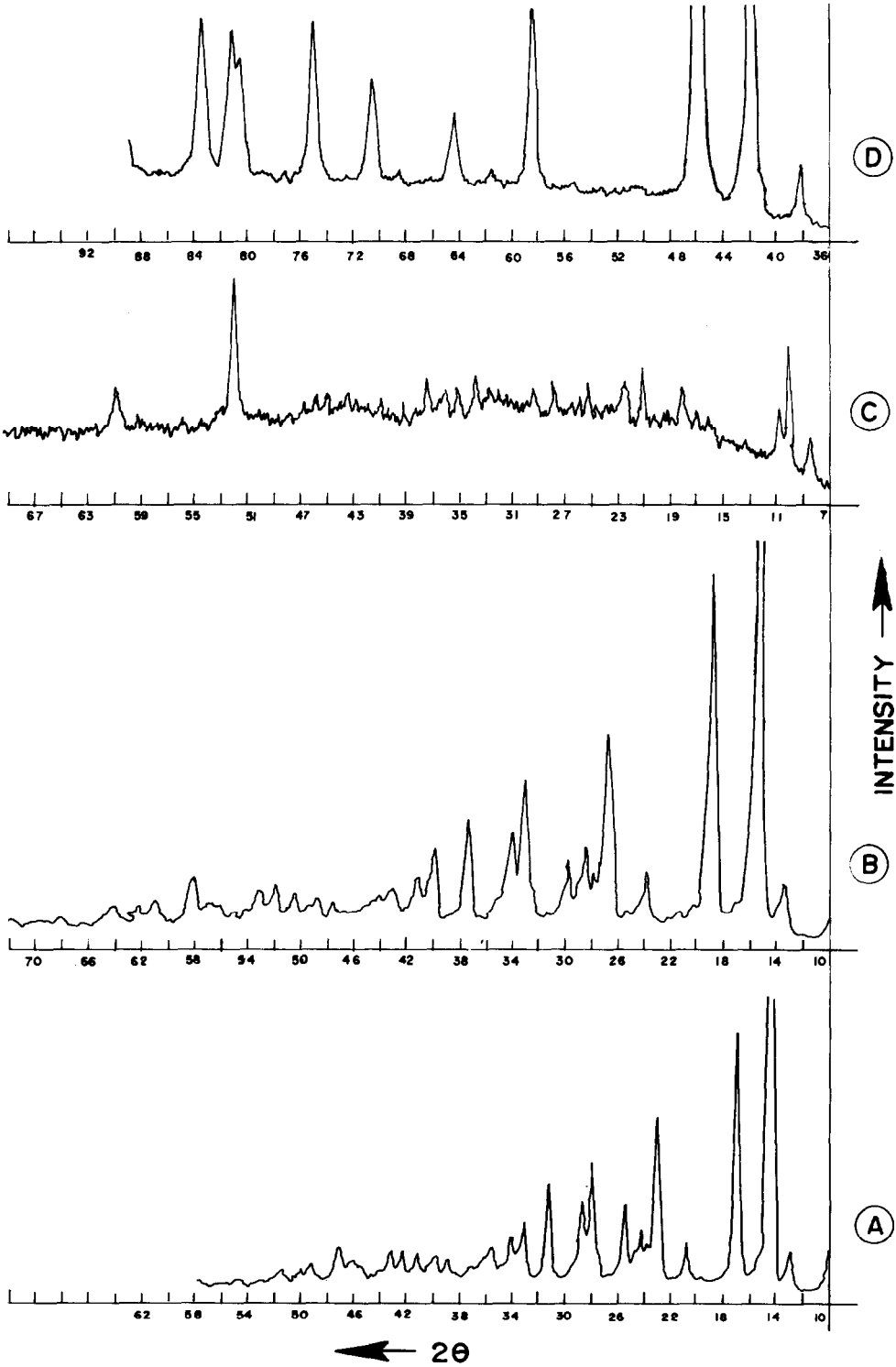

Fig. 3. X-ray powder diffractograms: A, $[Cu(en)_2(H_2O)_2]C_2O_4$: B, $[Cu(en)_2]C_2O_4$; C, $Cu(en)C_2O_4$; D, CuO.

TABLE 5

X-ray powder diffraction data for the final thermolysis product of $[Cu(en)_2(H_2O)_2]C_2O_4$

Experimental		JCPDS data for CuO	
d (Å)	I/I_0	d (Å)	I/I_0
2.7594	13.35	2.751	12
2.5338	92.57	2.523	100
2.3314	100.00	2.323	96
1.9638	16.00	1.959	3
1.8706	35.07	1.866	25
1.7866	16.88	1.778	2
1.7158	23.49	1.714	8
1.5868	26.07	1.581	14
1.5076	32.91	1.505	20
1.4124	25.03	1.418	12
1.3798	31.93	1.375	19

The X-ray diffraction patterns of the complex and the two intermediates are shown in Fig. 3. The major intensities along with the d spacing of the complex, intermediates and residue are given in Tables 5 and 6.

The area under the DSC curve for each stage is a measure of the heat of reaction. The calculated values of ΔH for each stage are also given in Table 4. The highest value of ΔH is for the dehydration reaction (stage I). An intermediate value is obtained for the deamination stage (stage II), and the lowest value is for the simultaneous deamination and decomposition reaction (stage III).

Kinetic parameters from non-mechanistic equations

The kinetic parameters evaluated for different stages of decomposition using non-mechanistic equations are given in Table 7 (TG) and Table 8 (DSC). The correlation coefficients (r) are in the range 0.9941–0.9997, indicating nearly perfect fits. It can be seen from these tables that the order parameter for different deamination stages is a decimal. It is known from the literature [21,22] that this apparent order, n, does not necessarily have to be an integer, but also a decimal.

From Tables 7 and 8, it can be seen that the kinetic parameters calculated with the Horowitz–Metzger equation are higher than the values from the other three equations. This is because of the inherent error involved in the approximation method employed in the derivation of the Horowitz–Metzger equation. The highest value of E is for stage III. An intermediate value is obtained for stage II and the lowest value is for stage I. For A the highest value is for stage II, the intermediate value for stage III and the lowest value for stage I. The same trend is also seen in the case of ΔS. The positive values

TABLE 6

X-ray powder diffraction data

$Cu[(en)_2(H_2O)_2]C_2O_4$		$Cu(en)_2C_2O_4$		$Cu(en)C_2O_4$	
d (Å)	I/I_0	d (Å)	I/I_0	d (Å)	I/I_0
6.1803	100.0	6.2531	100.0	2.0873	100.0
3.7969	35.74	5.2389	61.93	9.6694	76.38
3.1204	28.34	3.8031	44.98	4.8334	69.09
5.2220	26.51	3.1419	31.35	3.7316	64.38
2.7885	24.17	2.8053	26.42	4.0951	60.89
2.6238	17.63	4.2001	16.97	3.1031	60.44
3.4179	15.50	2.6288	16.30	2.9985	60.13
3.5946	15.24	1.8743	15.22	5.5909	60.13
2.5600	13.79	3.6069	15.11	4.5896	60.06
4.2070	12.44	2.0744	14.24	3.2739	56.87
1.8720	12.01	6.9689	14.14	1.8080	56.34
2.4498	11.11	2.5607	13.73	3.5558	56.26
2.0732	11.11	2.1331	12.79	2.9327	56.11
2.1921	10.35	2.4556	12.68	2.8272	55.88
2.0285	9.20	2.0347	11.91	2.4606	55.58
1.7943	8.95	3.2985	11.84	2.7112	53.22
2.1292	8.87	2.1941	10.73	3.2017	53.91
1.9022	8.05	1.8002	10.09	2.3304	52.99
1.7168	7.82	1.7179	9.75	4.0004	52.84
6.9380	7.80	2.3974	9.68	2.5965	52.69
2.3623	7.34	3.4367	9.58	2.3783	52.46
2.2354	6.89	1.7710	9.44	2.3017	52.16
1.6302	6.06	2.2622	9.31	3.9084	50.94
1.5893	5.79	4.8535	9.24	2.2742	49.81
		1.9101	9.24	9.1114	49.65
		1.6297	7.96	2.0518	49.05
		4.6081	7.55	5.8665	48.13
		1.6001	7.52	5.1853	46.54
				1.8536	45.93
				1.8673	45.70
				5.0385	45.40
				6.2106	45.17
				2.0049	44.49
				1.9616	44.41
				1.7269	43.35
				1.9193	42.74
				1.7613	42.06

of ΔS indicate that the activated complexes for all the stages of decomposition have a less ordered structure compared with the reactant, and the reaction in these cases may be described as faster than normal [23].

The kinetic parameters evaluated for different stages of decomposition from the TG and DSC curves may be compared (Tables 7 and 8). The values

TABLE 7

Kinetic parameters for the decomposition of diaquobis(ethylenediamine)copper(II) oxalate using non-mechanistic equations from TG data

		Stage I	Stage II	Stage III
n		1.12	1.11	0.98
E	CR	133.23	199.93	208.60
(kJ mol^{-1})	MT	131.65	200.40	210.08
	HM	147.18	215.38	228.22
	MKN	133.35	199.98	208.67
A	CR	1.91×10^{17}	8.01×10^{20}	1.03×10^{19}
(s^{-1})	MT	1.03×10^{17}	8.25×10^{20}	1.39×10^{19}
	HM	1.87×10^{19}	4.57×10^{22}	9.73×10^{20}
	MKN	1.99×10^{17}	8.17×10^{20}	1.05×10^{19}
ΔS	CR	84.11	151.63	114.46
(J K^{-1} mol^{-1})	MT	79.02	151.88	116.90
	HM	122.21	185.26	152.23
	MKN	84.46	151.80	114.64
r	CR	0.9977	0.9969	0.9997
	MT	0.9979	0.9971	0.9997
	HM	0.9977	0.9963	0.9991
	MKN	0.9978	0.9969	0.9996

CR, Coats–Redfern; MT, MacCallum–Tanner; HM, Horowitz–Metzger; MKN, Madhusudanan–Krishan–Ninan.

TABLE 8

Kinetic parameters for the decomposition of diaquobis(ethylenediamine)copper(II) oxalate using non-mechanistic equations from DSC data

		Stage I	Stage II	Stage III
n		1.12	1.11	0.98
E	CR	133.41	189.67	289.57
(kJ mol^{-1})	MT	132.02	190.06	291.64
	HM	144.28	208.76	302.66
	MKN	133.49	189.79	289.59
A	CR	0.62×10^{17}	0.50×10^{20}	0.49×10^{28}
(s^{-1})	MT	0.35×10^{17}	0.50×10^{20}	0.88×10^{28}
	HM	0.20×10^{19}	0.73×10^{22}	0.10×10^{30}
	MKN	0.64×10^{17}	0.52×10^{20}	0.50×10^{28}
ΔS	CR	74.62	128.63	280.85
(J K^{-1} mol^{-1})	MT	70.04	128.57	285.69
	HM	103.47	170.03	306.38
	MKN	74.85	128.93	281.00
r	CR	0.9973	0.9942	0.9986
	MT	0.9975	0.9946	0.9987
	HM	0.9974	0.9941	0.9975
	MKN	0.9972	0.9943	0.9996

CR, Coats–Redfern; MT, MacCallum–Tanner; HM, Horowitz–Metzger; MKN, Madhusudanan–Krishan–Ninan.

for stages I and II, evaluated using the two techniques, agree very well. However, the kinetic parameters for the third stage of decomposition, calculated using the DSC analysis, are higher than the corresponding values obtained from the TG data. There is no unambiguous explanation for the larger difference observed in the third stage; however, one probable reason can be the overlapping of two different types of reactions (reversible deamination and irreversible decomposition of oxalate). Earlier observations in our laboratories have also shown that quantitative correlations are better for reversible reactions than for irreversible reactions [2,24].

TABLE 9

Kinetic parameters for the decomposition of diaquobis(ethylenediamine)copper(II) oxalate using mechanistic equations from TG data

Mechanistic equation		Stage I	Stage II	Stage III
1	E	189.36	297.05	333.60
	A	7.85×10^{24}	3.18×10^{31}	1.38×10^{31}
	r	0.98375	0.97830	0.98661
2	E	209.00	322.53	357.20
	A	3.64×10^{27}	1.79×10^{34}	2.33×10^{33}
	r	0.98988	0.98619	0.99236
3	E	234.30	356.31	390.24
	A	5.20×10^{30}	4.28×10^{37}	1.75×10^{36}
	r	0.99527	0.99335	0.99795
4	E	217.31	333.53	367.84
	A	1.44×10^{28}	8.20×10^{34}	7.11×10^{33}
	r	0.99207	0.98904	0.99462
5	E	127.85	193.12	209.83
	A	2.93×10^{16}	1.22×10^{20}	1.40×10^{19}
	r	0.99742	0.99666	0.99960
6	E	60.92	92.78	100.67
	A	4.55×10^{6}	2.85×10^{8}	9.00×10^{7}
	r	0.99721	0.99632	0.99954
7	E	38.61	59.34	64.29
	A	2.08×10^{3}	3.20×10^{4}	1.41×10^{4}
	r	0.99701	0.99603	0.99955
8	E	107.92	166.05	182.70
	A	1.36×10^{13}	3.37×10^{16}	8.42×10^{15}
	r	0.99277	0.98998	0.99553
9	E	114.14	174.38	190.88
	A	8.08×10^{13}	2.26×10^{17}	4.27×10^{16}
	r	0.99501	0.99303	0.99783

E, kJ mol^{-1}; A, s^{-1}.

Choice of reaction mechanism

The TG and DSC data were analysed using the nine mechanistic equations given in Table 2. The reaction mechanism is inferred from the equation that gives the best representation of the experimental data. The r values, along with the values of E and A obtained from the slope and intercept respectively, for the nine equations are given in Table 9 (for TG) and Table 10 (for DSC). From these tables, it can be seen that the highest value of r

TABLE 10

Kinetic parameters for the decomposition of diaquobis(ethylenediamine)copper(II) oxalate using mechanistic equations from DSC data

Mechanistic equation		Stage I	Stage II	Stage III
1	E	176.53	405.59	347.02
	A	2.15×10^{22}	3.07×10^{44}	1.21×10^{33}
	r	0.97810	0.98818	0.97418
2	E	197.82	414.19	399.08
	A	1.46×10^{25}	1.70×10^{45}	1.83×10^{38}
	r	0.98743	0.98927	0.98491
3	E	227.03	423.24	472.71
	A	6.14×10^{28}	4.74×10^{45}	2.11×10^{45}
	r	0.99540	0.99057	0.99511
4	E	207.28	417.25	422.90
	A	7.90×10^{25}	8.90×10^{44}	1.28×10^{40}
	r	0.99071	0.98983	0.98902
5	E	126.82	212.42	273.76
	A	6.66×10^{15}	2.83×10^{22}	1.19×10^{26}
	r	0.99768	0.99110	0.99962
6	E	60.30	102.52	132.62
	A	2.09×10^{6}	4.66×10^{9}	2.96×10^{11}
	r	0.99731	0.99040	0.99965
7	E	38.13	65.91	85.55
	A	1.21×10^{3}	2.17×10^{5}	3.37×10^{6}
	r	0.99698	0.99000	0.99929
8	E	103.22	205.69	213.98
	A	1.07×10^{12}	2.11×10^{21}	2.96×10^{19}
	r	0.99188	0.98958	0.99084
9	E	110.41	207.94	232.07
	A	8.35×10^{12}	2.66×10^{21}	1.61×10^{21}
	r	0.99501	0.99023	0.99487

E, kJ mol^{-1}; A, s^{-1}.

for all stages of decomposition is obtained for the Mampel equation (eqn. 5), except for the DSC data for the third stage of decomposition for which the best fit curve is obtained with eqn. (6). However, the difference in r between eqns. (5) and (6) in this case is only negligible small (i.e. 3×10^{-5}). Moreover, eqn. (5) yields results of E and A which are closer to the values from the non-mechanistic equations.

It can also be seen from Tables 9 and 10 that some more equations give good linear curves with high values of r, though not as high as eqn. (5). Therefore, it may become difficult to assign the reaction mechanism unequivocally from the linearity of the kinetic curves alone. In such cases, the operating mechanism can also be chosen by comparing the kinetic parameters with those obtained by non-mechanistic equations [25]. In the present case a comparison with the values obtained by the Coats–Redfern method will be more appropriate, as the same method was used here for solving the exponential integral. The kinetic parameters calculated for the three stages of decomposition using the Coats–Redfern equation may be compared with the values of E and A obtained from the mechanistic equations (Tables 9 and 10). It can be seen that, for the different stages of decomposition, the kinetic parameters obtained from the Coats–Redfern equation are in good agreement with the values obtained from the Mampel equation for both TG and DSC. Thus, we can infer that the rate-controlling process for the reaction is random nucleation with the formation of one nucleus on each particle.

ACKNOWLEDGEMENTS

We thank the authorities of Vikram Sarabhai Space Centre for providing the instrumental facilities. The help of Dr. K. Krishnan and G. Viswanathan Asari with the TG/DSC instrumental work is gratefully appreciated, as is the aid of A. Natarajan in the X-ray diffraction work.

REFERENCES

1 W.W. Wendlandt, Thermal Analysis, Wiley-Interscience, New York, 3rd edn., 1986.
2 C.G.R. Nair and K.N. Ninan, Thermochim. Acta, 23 (1978) 161.
3 K.N. Ninan and C.G.R. Nair, Thermochim. Acta, 37 (1980) 161.
4 J.E. House, Jr. and J.C. Bailar, J. Am. Chem. Soc., 91 (1969) 67.
5 C.G.R. Nair and P.M. Madhusudanan, Thermochim. Acta, 14 (1976) 373.
6 W.W. Wendlandt and J.P. Smith, The Thermal Properties of Transition Metal Ammine Complexes, Elsevier, Amsterdam, 1967, p. 132..
7 S. Mathew, C.G.R. Nair and K.N. Ninan, Thermochim. Acta, 144 (1989) 33.
8 J.M. Haschke and W.W. Wendlandt, Anal. Chim. Acta, 32 (1965) 386.
9 A.W. Coats and J.P. Redfern, Nature, 201 (1964) 68.

10 J.R. MacCallum and J. Tanner, Eur. Polym. J., 6 (1970) 1033.
11 H.H. Horowitz and G. Metzger, Anal. Chem., 35 (1963) 1464.
12 P.M. Madhusudanan, K. Krishnan and K.N. Ninan, Thermochim. Acta, 97 (1986) 189.
13 J. Sestak and G. Berggren, Thermochim. Acta, 3 (1971) 1.
14 V. Satava, Thermochim. Acta, 2 (1971) 423.
15 M.D. Juddo and M.T. Pope, J. Therm. Anal., 4 (1972) 31.
16 J. Zsako, J. Therm. Anal., 5 (1973) 239.
17 V.M. Gorbachev, J. Therm. Anal., 8 (1975) 349.
18 A.B.P. Lever, Inorg. Chem., 10 (1971) 817.
19 J.E. House, Jr. and F.M. Tahir, Thermochim. Acta, 118 (1987) 191.
20 Hannewalt Method Search Manuel, International Center for Diffraction Data, JCPDS, Swarthmore, PA., p. 748.
21 D. Blecic and Z.D. Zivkovic, Thermochim. Acta, 60 (1983) 68.
22 A.C. Norris, M.I. Pope and M. Selwood, Thermochim. Acta, 41 (1980) 357.
23 A.A. Frost and R.G. Pearson, Kinetics and Mechanism, Wiley, New York, 1961, p. 101.
24 A. Alloun and C.G.R. Nair, Thermochim. Acta, 92 (1985) 767.
25 P.H. Fong and D.T. Chen, Thermochim. Acta, 18 (1977) 273.